ACS APPLIED MATERIALS & INTERFACES

Research Article

www.acsami.org

Ni_2P Nanosheets/Ni Foam Composite Electrode for Long-Lived and pH-Tolerable Electrochemical Hydrogen Generation

Yanmei Shi, You Xu, Sifei Zhuo, Jingfang Zhang, and Bin Zhang*

Department of Chemistry, School of Science, Tianjin University, and Collaborative Innovation Center of Chemical Science and Engineering (Tianjin), 92th Weijin Road, Tianjin 300072, China

Supporting Information

ABSTRACT: The continuous consumption of fossil fuels and accompanying environmental problems are driving the exploration of low-cost and effective electrocatalysts to produce clean hydrogen. A Ni_2P nanosheets/Ni foam composite, as a non-noble metal electrocatalyst, has been prepared through a facile chemical conversion pathway using surface oxidized Ni foam as precursor and low concentration of trioctylphosphine (TOP) as a phosphorus source. Further investigation shows the oxidized layer of Ni foam can orient the formation of Ni_2P nanosheets and facilitate the reaction with TOP. The Ni_2P/Ni, acting as a robust 3D self-supported superaerophobic hydrogen-evolving cathode, shows superior catalytic performance, stability, and durability in aqueous media over a wide pH value of 0−14, making it a versatile catalyst system for hydrogen generation. Such highly active, stable, abundant, and low-cost materials hold enormously promising potential applications in the fields of catalysis, energy conversion, and storage.

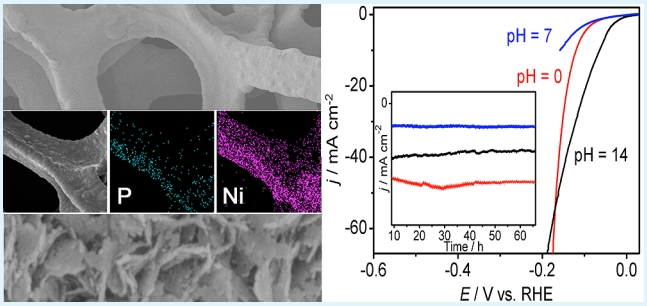

KEYWORDS: *electrocatalysts, hydrogen evolution, nanomaterials, self-supported, transition metal phosphide*

1. INTRODUCTION

Realization of the hydrogen economy paradigm in the future will require efficient and sustainable production of hydrogen.[1−5] Electrocatalytic hydrogen evolution reaction (HER) is considered to be one of promising strategies for hydrogen generation from water splitting.[6−9] A key challenge for electrochemical HER is the exploration of low-cost and highly efficient electrocatalysts with low overpotential and long-term stability. Recently, some solid-state inorganic materials including metal alloys,[10] borides,[11] carbides,[11,12] nitrides,[13−15] sulfides,[16−22] selenides,[23] and even metal free catalysts[24] have been found to electrochemically active for HER. In particular, transition metal phosphide nanostructured materials with structural and electronic analogies to the active site of hydrogenase have been identified as active HER catalysts because they could merge the activity of hydrogenase with the stability of a heterogeneous catalyst.[25,26] In our previous work, we have reported the anion-exchange synthesis of FeP porous nanosheets and demonstrated its high electrocatalytic activity for HER.[27] Schaak's, Lewis', and Hu's groups have reported the preparation of Ni_2P as an efficient electrocatalyst for HER.[25,28] Subsequently, a variety of transition metal phosphide nanomaterials has been investigated and characterized as potential HER catalysts.[29−38] Despite the advances of solid-state HER catalysts, the development of high efficient and stable electrocatalysts in aqueous media over a wide pH range is highly desirable.[33,39,40]

In practical applications, the construction of ideal electrodes by optimizing the structural, mechanical, and electrical contact between the catalyst and electrode substrates is a key issue for achieving an excellent catalytic activity and stability.[41] Currently, the HER electrocatalysts are usually assembled on two-dimensional (2D) planar substrates through a variety of methods, such as electrodeposition, sputtering, dip-coating, and spin-coating, to form HER cathodes.[41,42] Compared to the conventional 2D planar architecture, self-supported hydrogen-evolving electrodes based on 3D porous materials might offer a large electroactive surface and thus improve the activity.[43,44] Taking advantage of comparatively large surface area, high electron conductivity, and low cost, Ni foam is usually used as an electrode material in applications such as electrocatalysis.[41,44−47] Recently, Zhang et al. have demonstrated the preparation of Ni_3S_2 nanorods/Ni foam composite electrode with high activity for electrocatalytic oxygen evolution.[44] Despite these important advances, the construction of a solid-state nickel-based catalyst grown directly on Ni foam as robust HER cathodes, to the best of our knowledge, has not been reported yet.

Over the past several years, a lot of strategies have been developed for the synthesis of metal phosphides. Recently, literature on thermal reaction of NaH_2PO_2 with an as-synthesized precursor at a relatively low temperature (ca. 300 °C) is booming.[28,29,31,35,36] Meanwhile, many strategies still focus on the reactions of trioctylphosphine (TOP) as a

Received: October 10, 2014
Accepted: January 7, 2015
Published: January 7, 2015

DOI: 10.1021/am5069547
ACS Appl. Mater. Interfaces 2015, 7, 2376−2384

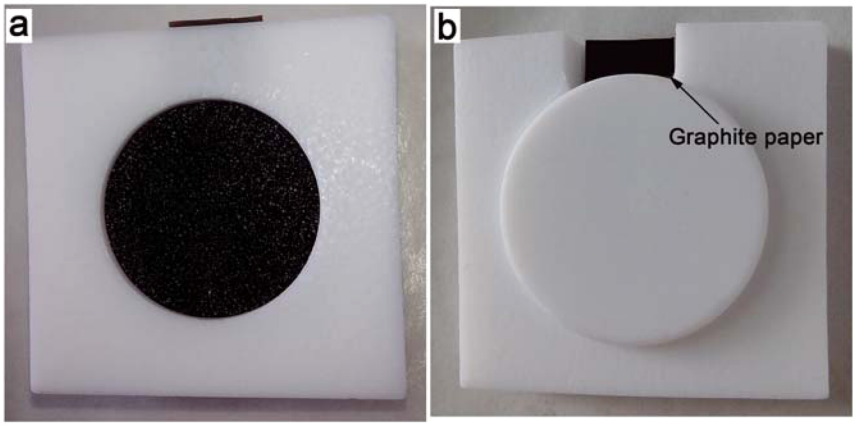

Figure 1. Front (a) and back (b) optical images of a piece of Ni_2P/Ni foam incorporated Teflon mold.

phosphorus source and solvent with organometallic complexes.[25,37,38,48,49] However, both of the methods have their inherent disadvantages. The highly concentrated TOP is toxic and flammable at elevated temperature, and the products often cannot achieve a unique morphology and structure without an additive. On the other hand, when heating NaH_2PO_2 over 200 °C, the highly toxic and flammable PH_3 will be generated in large amounts,[50,51] and thus a more complicated setup and post-treatment procedure are required in most cases. Very recently, vertical nanosheets materials on substrate have been proved to provide a superaerophobic surface, resulting in promoting the electrocatalytic performance.[52] To obtain vertical nanosheets materials with a superaerophobic surface, the general use of NaH_2PO_2 as a phosphorus source often need two steps, i.e., electrodeposition and thermal reaction, making the process complicated. Therefore, the efficient synthesis of metal phosphides through a simple way with specific morphology and structure is still highly desirable.

Herein, we report the fabrication of a highly active and long-lived HER cathode formed by growing Ni_2P nanosheets directly on Ni foam via a facile method (referred to as Ni_2P/Ni) by using low concentration of TOP. The resulting Ni_2P/Ni, as a robust 3D hydrogen-evolving cathode, shows a low onset overpotential of 80 mV and a small Tafel slope of 68 mV dec^{-1}, and it could maintain its catalytic activity for over 65 h in acidic media. Furthermore, this Ni_2P/Ni electrode offers excellent catalytic stability and performance under neutral and alkaline condition, making it a versatile catalyst for HER.

2. EXPERIMENTAL SECTION

2.1. Synthesis of the Ni_2P/Ni Composite. The Ni foams were cut into circular shapes with a diameter of 2.5 cm. Prior to the synthesis, the circular Ni foams were soaked in acetone and 1 M HCl for 5 min in sequence to remove the organic molecules and the oxide layer. After that, the Ni foams were washed with deionized water and ethanol and then exposed to the air for at least 3 days to form an oxidized surface. For a typical synthesis, two pieces of the Ni foams, 15 mL of 1-octadecene, and 1 mL of TOP were placed in a three-neck flask equipped with a glass covered magnetic stirring bar and a condenser with an air-flow adapter on top. The three-neck flask was then degassed under vacuum at 100 °C for about 15 min, and then the flask was heated to 320 °C and kept refluxing for 2 h. The reaction was then allowed to cool down to room temperature. The black products were picked out of the flask and washed several times with hexane and ethanol, respectively, then the product was dried naturally.

2.2. Characterization. The scanning electron microscopy (SEM) images, energy-dispersive X-ray spectroscopic analysis (EDS), and elemental distribution mapping were taken with a Hitachi S-4800 scanning electron microscope equipped with the Thermo Scientific energy-dispersion X-ray fluorescence analyzer. Transmission electron microscopy (TEM) and high-resolution transmission electron microscopy (HRTEM) images were carried out with a JEOL JEM-2100F microscope. Prior to the TEM and HRTEM measurements, a piece of Ni_2P/Ni foam was immersed in ethanol in a centrifugal tube and was under ultrasonic continuously for more than 6 h. After that, the black precipitate was isolated through centrifugation and dried in a vacuum oven at 30 °C for 6 h. The X-ray diffraction (XRD) patterns were recorded with a Panalytical X'Pert Pro diffraction system with a Co Kα source (λ = 1.78897 Å), then the data were converted to that corresponding to the Cu Kα source by Bragg's law. To improve the crystallization, the Ni_2P exfoliation was calcinated at 500 °C for 2 h in argon atmosphere. X-ray photoelectron spectroscopy (XPS) was performed using a PerkinElmer PHI 1600 Versa Probe.

2.3. Electrochemical Measurements. All electrochemical measurements were performed using an electrochemical workstation (CHI 660D, CH Instruments, Austin, TX) in a three-electrode system. The Ni_2P/Ni can be used as working electrode directly. To get accurate reaction area, a Teflon mold with a defined exposed area was utilized. The edge of Ni_2P/Ni was sealed with the epoxy resin before setting in the mold. As shown in Figure 1, the diameter of the circular exposed area was 2.1 cm. A piece of graphite paper was used to connect the Ni_2P/Ni foam with the external circuit through a metal alligator clip. All the potentials referred to in this paper are against a reverse hydrogen electrode (RHE).

Before the electrochemical measurement, the electrolyte was degassed by bubbling argon for 30 min. When the electrolyte was 0.5 M H_2SO_4, a Pt sheet and a saturated calomel electrode (SCE) were used as counter and reference electrodes, respectively. The reference electrode was calibrated in H_2 saturated electrolyte with respect to an in situ RHE. Another Pt sheet was used as a working electrode. The polarization curves were obtained by sweeping the potential from 0.02 to −0.43 V in 0.5 M H_2SO_4, with a sweep rate of 5 mV/s. The polarization curves were replotted as overpotential (η) versus log current density (log j/[j]) to get Tafel plots for quantification of the HER activities of investigated catalysts. The cyclic voltammetry (CV) plots were swept between 0 and −0.17 V in 0.5 M H_2SO_4 with the scanning rate of 100 mV/s. The current density-time (I–t) curves were measured at a constant potential of −0.15 V in 0.5 M H_2SO_4. The electrochemical impedance spectroscopy (EIS) was carried out at the overpotential of 120 mV in 0.5 M H_2SO_4 from 10000 to 0.01 Hz at an amplitude of 5 mV.

To collect the H_2 produced from the cathode in 0.5 M H_2SO_4, a more negative potential of −0.23 V was used. The evoluted H_2 was collected by a water–gas displacing method, which was achieved by an upside-down buret filling up with water. The end of the buret without the cock was immersed under water with the cock shutting off. The volume of hydrogen could be read out from the scale on the buret directly.

DOI: 10.1021/am5069547
ACS Appl. Mater. Interfaces 2015, 7, 2376–2384

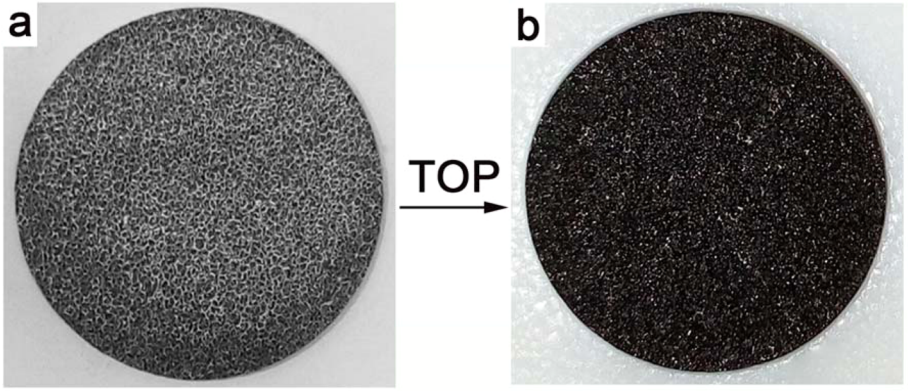

Figure 2. Optical images of bare Ni foam (a) and the converted products after treated with TOP at elevated temperature (b).

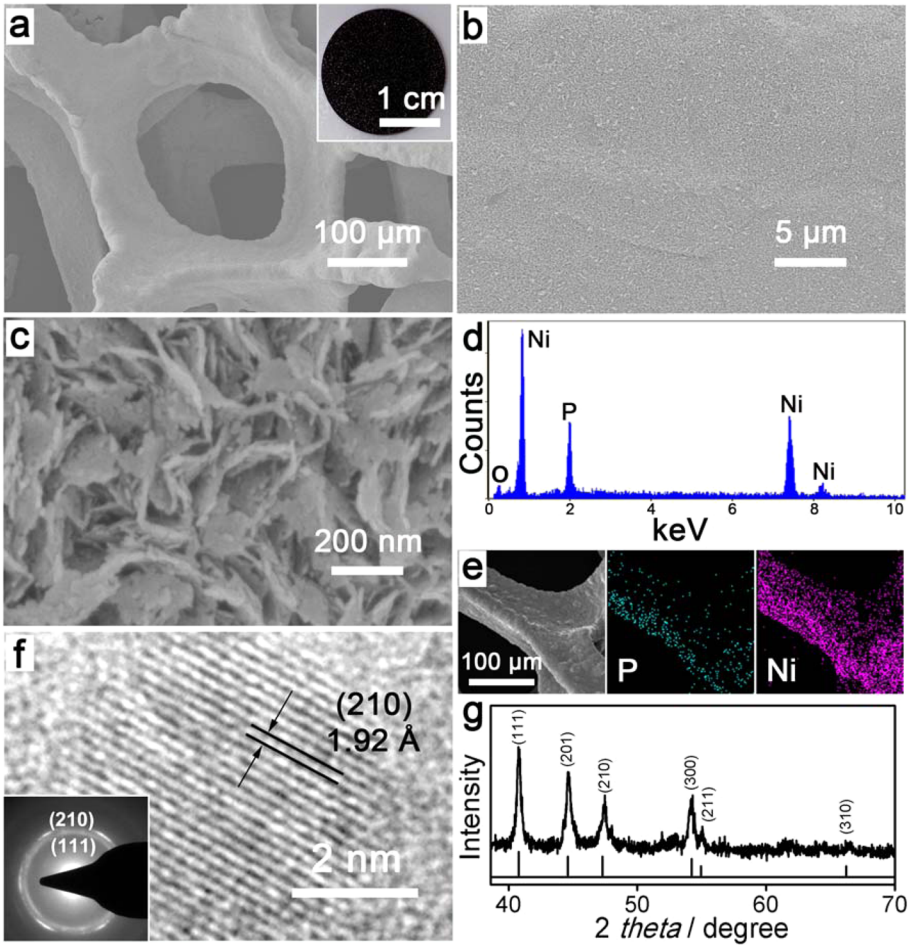

Figure 3. Low (a,b) and high (c) magnification SEM images, (d) EDS spectrum, (e) elemental distribution mapping of the Ni_2P/Ni foam. The inset of (a) is the optical image of Ni_2P/Ni in the Teflon mold. (f) The HRTEM image of the Ni_2P exfoliation. The inset of (f) is the corresponding SAED pattern. (g) XRD pattern of the Ni_2P exfoliation calcinated at 500 °C in argon for 2 h.

When 0.5 M phosphate buffer solution (PBS) was used as electrolyte, the SCE still served as the reference electrode. The polarization curves were obtained by sweeping the potential from 0.10 to −0.45 V with the same scanning rate of 5 mV/s. The *I*−*t* curve was measured at a constant potential of −0.22 V.

While the pH of the electrolyte was 14, 1 M KOH aqueous solution was employed. The reference electrode was replaced by a Hg/HgO electrode with the inner reference electrolyte of 1 M KOH. The sweeping range of the polarization curves was 0.22 to −0.37 V with the scanning rate of 5 mV/s. The *I*−*t* curve was measured at a potential of −0.07 V.

3. RESULTS AND DISCUSSION

3.1. Morphology and Structure. The Ni_2P/Ni composite was prepared through a facile chemical conversion method at elevated temperature using Ni foam with oxidized surface as the starting material and low concentration of TOP (Supporting Information, Table S1) as the phosphorus source (Figure 2). Parts a−c of Figure 3 show SEM images of the as-obtained Ni_2P/Ni. The skeleton of the Ni foam was not changed, while the color changed from silver-gray to black, suggesting that the

DOI: 10.1021/am5069547
ACS Appl. Mater. Interfaces 2015, 7, 2376−2384

surface of the Ni foam was converted into metal phosphides. Upon closer observation of the high-magnification SEM image, it was found that the foam is uniformly covered by numerous nanosheets with a lateral size of 400−500 nm and a thickness of ∼20 nm (see Figure S2 in the Supporting Information). EDS point-scan spectrum and EDS elemental mapping indicate that Ni and P are the main elemental components and are uniformly distributed on the whole skeleton (Figure 3d,e).

To further investigate the morphology and microstructure of the nanosheets gown on the Ni foam, the as-obtained Ni_2P/Ni composite was sonicated continuously for 6 h to exfoliate some nanosheets from the Ni foam. TEM images further verify their sheet-like morphology (Supporting Information, Figure S3). The HRTEM image clearly shows these nanosheets consist of thin amorphous layers, loaded with tiny crystalline particles with an average diameter of ∼5 nm (Figure 3f). Figure 3f also shows lattice fringes of 1.92 Å, corresponding to the (210) interplanar spacings of Ni_2P. The only two bright rings displayed in the selective area electron diffraction (SAED) pattern (inset of Figure 3f), which can be indexed to (111) and (210) facets of hexagonal Ni_2P, also revealed the poor crystallinity and polycrystalline nature of the as-prepared Ni_2P. EDS spectrum of the exfoliated Ni_2P nanosheets shows these nanosheets consist of P and Ni with an atom ratio of Ni:P close to 2:1 (Supporting Information, Figure S4). Taking the poor crystallinity of the as-prepared Ni_2P (Figure 4) into consideration, a typical XRD pattern (Figure 3g) was obtained after calcinating the Ni_2P exfoliation at 500 °C in argon for 2 h. All of the diffraction peaks matches very well with hexagonal Ni_2P (JCPDS 03-0953). XPS is used to analyze the surface composition of the composite electrode (Figure 5). The peak position and the shape of the envelopes matched well with the reported Ni_2P rather than other nickel phosphides (Supporting Information, Table S2).[53−59] In the P 2p core level spectrum, the peak at 129.5 eV has been reported for $P^{\delta-}$ on metal phosphides, and the peak at 133.1 eV for surface metal phosphate species, due to the superficial oxidation of Ni_2P[59] Ni $2p_{2/3}$ core level spectrum involves two contributions as well.[59] The peak centered at 853.1 eV is assigned to $Ni^{\delta+}$ in the Ni_2P phase. Another peak at 857.0 eV corresponds to the Ni^{2+} ions interacting possibly with phosphate ions as a consequence of a superficial oxidation. The broad satellite peak (centered at 862.5 eV) at approximately 6 eV above the Ni^{2+} species is the shakeup peak of divalent Ni^{2+} species.[59] The peak corresponding to the zerovalent nickel was not found, which implied the surface of the as-prepared Ni_2P/Ni is fully covered with Ni_2P. No exposure of the metal nickel skeleton contributes to the super stability and durability of the as-prepared Ni_2P/Ni electrode in the electrocatalytic measurements. These results indicate that Ni_2P nanosheets are grown on the surface of Ni foam through reacting with a low concentration of TOP at elevated temperature, forming 3D self-supported Ni_2P nanosheets/Ni foam composite.

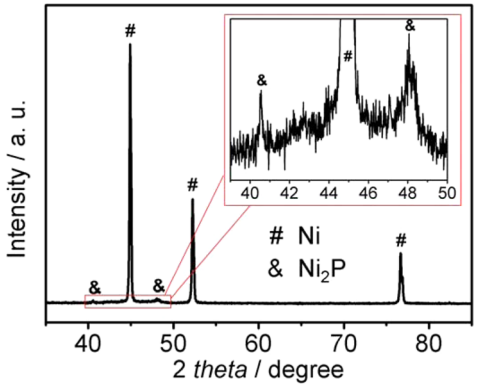

Figure 4. XRD pattern of the as-prepared Ni_2P/Ni foam before being calcinated at 500 °C in argon. The peak labeled by "&" corresponds to the (111) and (210) facets of Ni_2P, respectively.

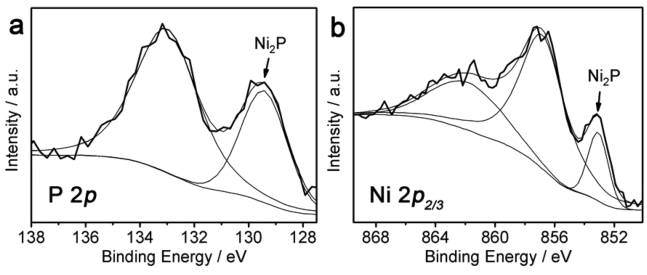

Figure 5. XPS spectra of P 2p core level (a) and Ni $2p_{2/3}$ core level (b) of the as-prepared Ni_2P/Ni.

3.2. Growth Mechanism. In a previous report, Schaak and co-workers have shown an efficient conversion to Ni_2P by reacting H_2-reduced Ni foil with TOP as solvent.[49] However, they did not obtain nanosheets structure, which might imply the oxidized layer on the surface of Ni foam in our case was the key to form Ni_2P nanosheets. To verify the hypothesis, a fresh HCl-treated Ni foam was taken to immediately react with TOP. After reaction, the color of the Ni foam turned dark-gray rather than black. Moreover, the resultant did not form nanosheets, with the very low content of phosphorus (Ni:P = ∼42:1) (Figure 6). The incomplete conversion in the low concentration of TOP (Supporting Information, Table S1) in turn implied the oxidized surface could facilitate the reaction with TOP and orient the formation of the nanosheets. Because the ultrathin oxidized layer was difficult to characterize (Supporting Information, Figure S1), a long-time-stored Ni foam with severely oxidized surface was employed to verify the composition of the oxidized layer. A typical SEM image of the severely oxidized Ni foam showed many tiny nanosheets distributed irregularly on the surface of the Ni foam (Figure 7a). The XPS spectra of Ni $2p_{2/3}$ core level of a piece of severely oxidized Ni foam are shown as Figure 7b. The peak position and the shape of the envelopes matched well with the reported nickel hydroxide,[60] which might imply the oxidized layer was composed of nickel hydroxide. According to above discussion, the chemical transformation mechanism can be speculated as following description. Prior to treating the Ni foam with TOP, a thin nickel hydroxide layer, which was difficult to observe by SEM, formed on the surface of the Ni foam by reacting with oxygen and water vapor during exposure in the air.[61] The thin nickel hydroxide layer consisted of many tiny nanosheets on Ni foam substrate, which could orient the growth of the Ni_2P. At elevated temperature, nickel hydroxide could decompose to nickel oxide,[62] which could react with TOP as well to form Ni_2P and facilitate the reaction.[63] Without the nickel hydroxide layer, converting the surface of Ni foam would need a much higher concentration of TOP and could not lead to the production of nanosheets.

3.3. Electrochemical Characterization. Because the Ni foam retains its flexible skeleton, the Ni_2P/Ni composite can directly act as the working electrode. To get accurate area of the

DOI: 10.1021/am5069547
ACS Appl. Mater. Interfaces 2015, 7, 2376−2384

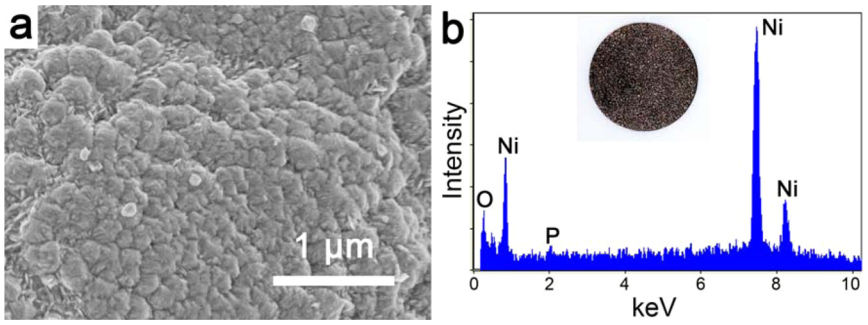

Figure 6. (a) SEM image and (b) EDS spectrum of a newly HCl-treated Ni foam reacted with TOP via the same reaction process. The molar ratio of Ni:P is about 42:1. The inset of (b) is optical image of the resultant products.

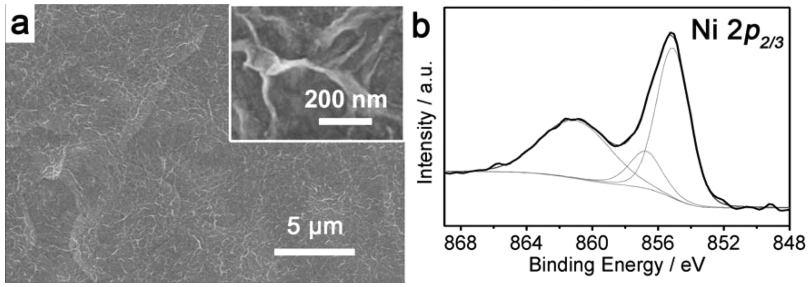

Figure 7. SEM images (a) and XPS spectra of Ni $2p_{2/3}$ core level (b) of a surface severely oxidized Ni foam exposed to air for 10 days. The inset of (a) is a corresponding high magnification SEM image.

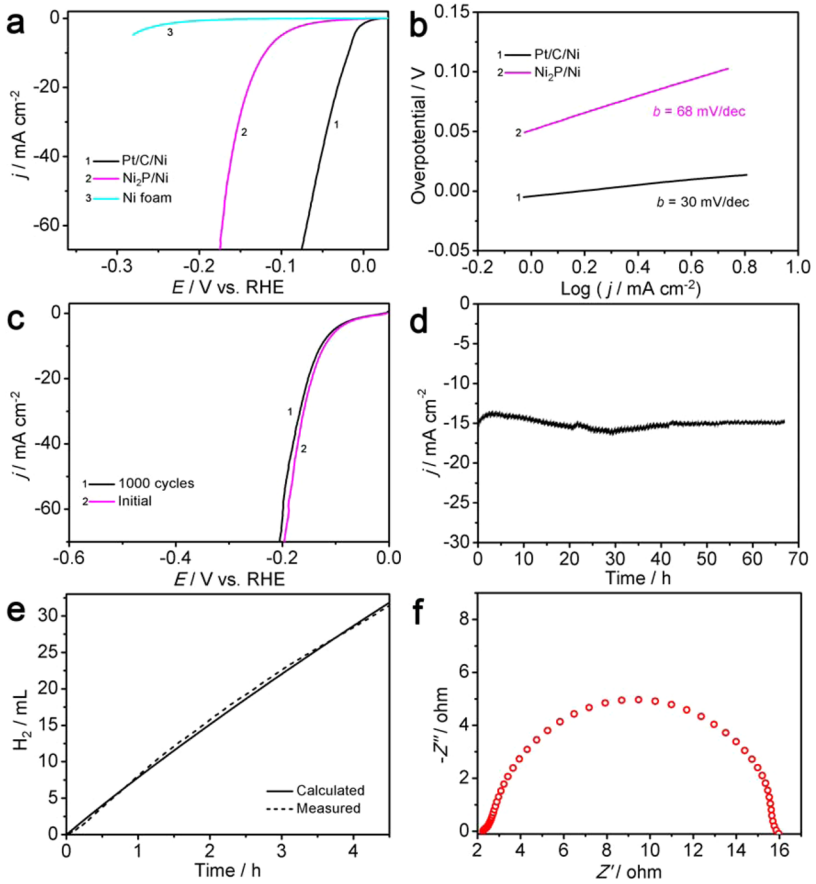

Figure 8. Electrocatalytic activities of the as-prepared Ni_2P/Ni electrode in 0.5 M H_2SO_4. (a) Polarization curves of Ni_2P/Ni, Pt/C/Ni, and bare Ni foam with a scan rate of 5 mV/s. (b) Tafel plots of Ni_2P/Ni and Pt/C/Ni. (c) Polarization curves of the as-obtained Ni_2P/Ni initially and after 1000 CV cycles. (d) Current density−time (I−t) curve of Ni_2P/Ni at the overpotential of 175 mV. (e) Current efficiency for H_2 evolution catalyzed by Ni_2P/Ni. (f) EIS spectrum of the as-obtained Ni_2P/Ni electrode at η = 120 mV in 0.5 M H_2SO_4. The data in (a−c) were iR corrected.

DOI: 10.1021/am5069547
ACS Appl. Mater. Interfaces 2015, 7, 2376−2384

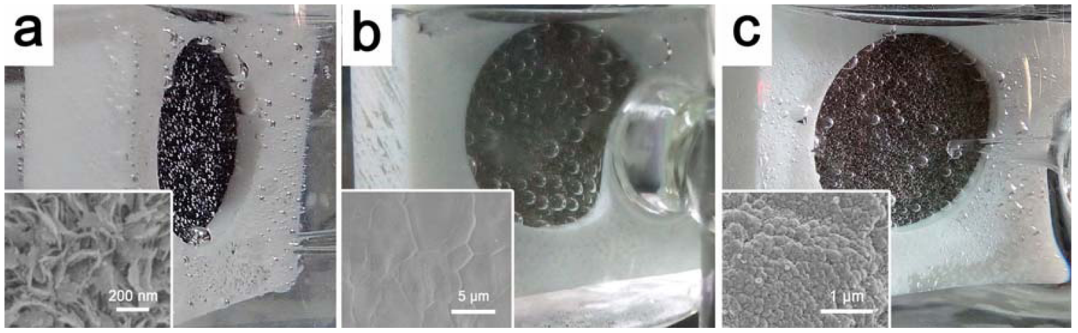

Figure 9. Optical images of (a) the Ni_2P/Ni, (b) Ni foam, and (c) a newly HCl-soaked Ni foam treated with TOP during the electrocatalytic measurements in 0.5 M H_2SO_4. The insets are the corresponding SEM images.

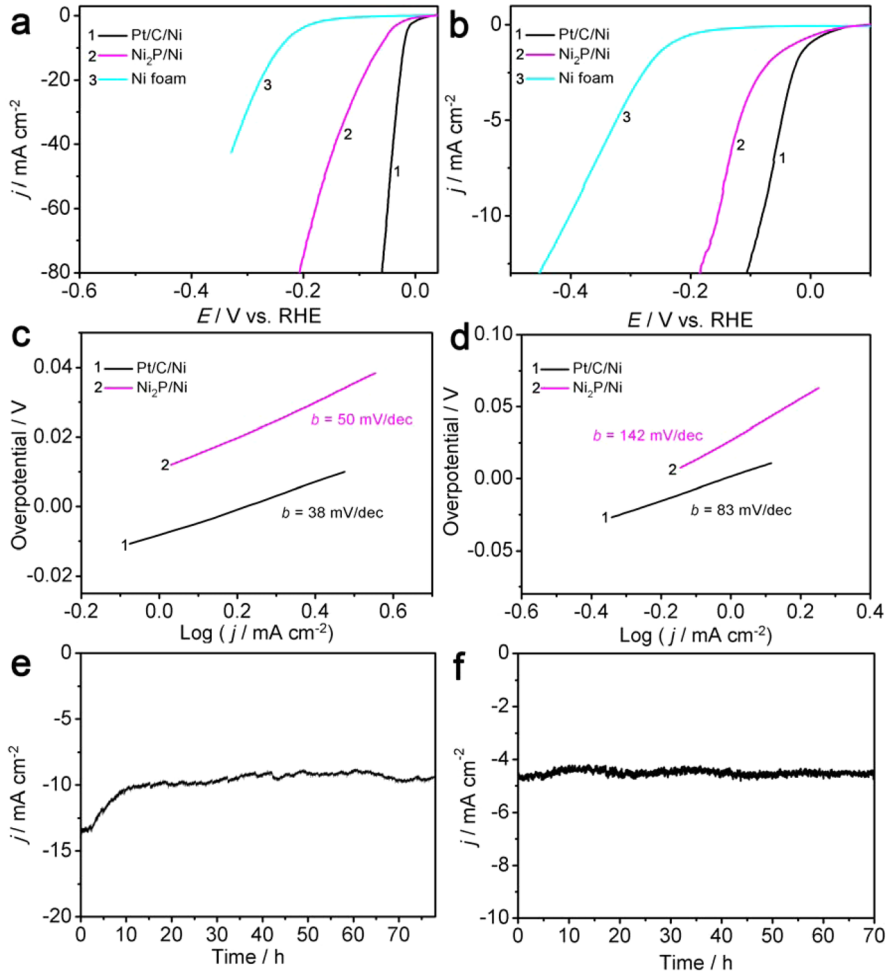

Figure 10. Electrocatalytic activities of the as-prepared Ni_2P/Ni electrode in 1 M KOH (a,c,e) and in 0.5 M PBS (b,d,f). (a,b) Polarization curves. (c,d) Tafel plots. (e,f) *I*–*t* curves. The data in (a–d) were *iR* corrected.

electrode, a Teflon mold with a specific exposed area was employed. The HER electrocatalytic activity of the as-prepared Ni_2P/Ni composite electrode was first evaluated in acidic media. Figure 8 shows the electrocatalytic activities of the as-prepared Ni_2P/Ni electrode in 0.5 M H_2SO_4. The performance of commercial Pt/C (20 wt %, Johnson Matthey) loading on Ni foam (referred to as Pt/C/Ni) and bare Ni foam were also examined for comparison. The polarization curves of these three electrodes are shown in Figure 8a. As expected, Pt/C/Ni electrode exhibited high HER catalytic activity with negligible overpotential. Although bare Ni foam showed poor HER activity, the Ni_2P/Ni electrode performed an onset overpotential of about 80 mV, which was compared favorably to many of the non-Pt HER catalysts in acidic media.[28,64,65] Further negative potential caused a rapid rise of cathodic current, suggesting Ni_2P/Ni acted as a high-performance 3D cathode for generating hydrogen from water. The measured Tafel slope of the Pt/C/Ni was about 30 mV dec^{-1} (Figure 8b), which is consistent with the reported values.[27] The Ni_2P/Ni electrode exhibited a small Tafel slope of about 68 mV dec^{-1} in the overpotential region of 50–120 mV. This Tafel slope

DOI: 10.1021/am5069547
ACS Appl. Mater. Interfaces 2015, 7, 2376–2384

reveals the HER might proceed via a Volmer–Heyrovsky mechanism.[66]

Durability and stability are very critical aspects to evaluate the performance of a catalyst in the practical applications. Durability of the catalytic response was evaluated by cycling the Ni_2P/Ni electrode continuously for 1000 cycles. After 1000 cycles, the polarization curve of the Ni_2P/Ni electrode nearly overlaps with the initial one, indicating a superior durability (Figure 8c). The stability of the Ni_2P/Ni electrode was further assessed in a longer-duration controlled potential electrolysis experiment. As shown in Figure 8d, the time dependent current density curve keeps steady at ~15 mA cm^{-2} for the whole electrolysis under a static applied potential of 175 mV, suggesting the Ni_2P/Ni electrode can maintain its catalytic activity for over 65 h. The hydrogen evolved from the cathode was collected by a water–gas displacing method. The volume–time curve of the collected H_2 was nearly the same as the one which was calculated according to the cumulative charge (Figure 8e), which meant the Faradaic efficiency of the catalyst was nearly 100%. It is worth mentioning that no obvious change in the morphology of the Ni_2P nanosheets was observed after the long-term stability test (Supporting Information, Figure S6).

Such high activity, stability, and durability for the Ni_2P/Ni electrode can be rationalized to the following aspects: (1) The loose arrangement of the Ni_2P nanosheets and the net-like skeleton of the Ni foam benefit the escape of the tiny bubbles. As shown in Figure 9, it could be found that the bubbles adsorbed on the Ni_2P/Ni foam (Figure 9a) were much smaller than those in the others, suggesting that the as-prepared Ni_2P nanosheets supported on Ni foam might own a superaerophobic surface, on which the adhesion of as-produced gas bubbles could be decreased, offering a rapid removal of small gas bubbles and constant working area.[52] Otherwise the bubbles will gather on the surface of the catalyst, decrease the active area, and hinder the ionic transportation. (2) The Ni_2P growing directly on the Ni foam also makes great contribution to the stability: (i) Growing directly leads to the strong chemical combination between the catalyst and the substrate, making the thin Ni_2P nanosheets not aggregate and not fall off easily due to bubbles escaping. (ii) The dense and uniform Ni_2P nanosheets could effectively resist the acidic corrosion to the Ni foam. (iii) Direct growth of Ni_2P on Ni foam can afford rapid electron transport from the Ni_2P to the electrode, which is very significant to increasing its HER activity. To glean this effect, an electrochemical impedance spectroscopy (EIS) was applied at an overpotential of 120 mV (Figure 8f). The Ni_2P/Ni electrode exhibited a very low impedance of ~14 Ω, which is much smaller than that collecting at the overpotential of 140 mV in 1 M H_2SO_4 by drop-casting the Ni_2P nanoparticles on the glassy carbon electrode in a previous report.[28] The reduced Faradaic impedance afforded markedly faster HER kinetics with the catalyst.[66]

Aiming to make the electrocatalytic H_2 evolution into large-scale applications, it is imperative to develop the electrocatalysts with high performance and good stability in the wide pH range of aqueous media. We further investigated the HER performance of the Ni_2P/Ni composite electrode in alkaline media. Figure 10a shows the polarization curve of the Ni_2P/Ni composite electrode in 1.0 M KOH (pH 14). Interestingly, the onset overpotential is about 41 mV and the Tafel slope is calculated to be 50 mV dec^{-1}, which are even better than those in acidic media (Figure 10a,c). Moreover, the Ni_2P/Ni electrode still exhibits excellent stability under such alkaline conditions (Figure 10e). Next, we investigated the HER performance of the Ni_2P/Ni electrode under neutral condition. In 0.5 M PBS (pH 7.03), it shows an onset HER overpotential of 78 mV and a Tafel slope of 142 mV dec^{-1} with excellent stability (Figure 10b,d,f). The poor Tafel slope may due to the HER's inherently slow kinetics in neutral media.[33] These results indicate that the as-prepared Ni_2P/Ni electrode shows a robust HER activity in aqueous reaction media over a wide pH range.

4. CONCLUSION

In summary, we developed a facile chemical conversion pathway to prepare Ni_2P nanosheets growing directly on the surface oxidized Ni foam as a composite electrocatalyst for HER. The whole fabrication process is simple, highly efficient, and easy to scale up, and the oxidized layer of Ni foam has been shown to orient the formation of Ni_2P nanosheets and facilitate the reaction with TOP. The as-obtained Ni_2P/Ni composite with the retention of flexible skeleton and 3D geometrical structure of Ni foam can be used directly as a hydrogen-evolution cathode. The Ni_2P/Ni electrode displays a high activity for HER with a low onset overpotential of 80 mV and a small Tafel slope of 68 mV dec^{-1} in acidic media. In addition, the Ni_2P/Ni electrode is also active for HER in both neutral and alkaline aqueous solutions. Furthermore, the as-obtained electrode can maintain the high performance for over 65 h in different pH aqueous solutions. Because the elements Ni and P are low-cost and abundant on the earth, the high activity and the long-lived stability make the Ni_2P/Ni composite a promising candidate for electrocatalysts for HER in large scale applications. Such highly active, abundant, and low-cost materials hold great promise for a variety of applications in the fields of catalysis, energy conversion, and storage.[67−70] Additionally, unexpected photochemical performance of metal phosphides and phosphorus may open up interesting possibilities to design and fabricate self-supported photoelectrodes composed of transition metal phosphides and/or their composites.[53,71,72]

■ ASSOCIATED CONTENT

Supporting Information

Experimental calculations, additional characterization, and electrochemical data. This material is available free of charge via the Internet at http://pubs.acs.org.

■ AUTHOR INFORMATION

Corresponding Author

*E-mail: bzhang@tju.edu.cn.

Notes

The authors declare no competing financial interest.

■ ACKNOWLEDGMENTS

This research was supported financially by the National Natural Science Foundation of China (nos. 21373149 and 21422104) and the Innovation Foundation of Tianjin University.

■ REFERENCES

(1) Dresselhaus, M. S.; Thomas, I. L. Alternative Energy Technologies. *Nature* **2001**, *414*, 332–337.

DOI: 10.1021/am5069547
ACS Appl. Mater. Interfaces 2015, 7, 2376–2384

(2) Walter, M. G.; Warren, E. L.; McKone, J. R.; Boettcher, S. W.; Mi, Q.; Santori, E. A.; Lewis, N. S. Solar Water Splitting Cells. *Chem. Rev.* **2010**, *110*, 6446−6473.
(3) Gray, H. B. Powering the Planet with Solar Fuel. *Nature Chem.* **2009**, *1*, 7−9.
(4) Vaneski, A.; Schneider, J.; Susha, A. S.; Rogach, A. L. Aqueous Synthesis of CdS and CdSe/CdS Tetrapods for Photocatalytic Hydrogen Generation. *APL Mater.* **2014**, *2*, 012104.
(5) Dai, F.; Zai, J.; Yi, R.; Gordin, M. L.; Sohn, H.; Chen, S.; Wang, D. Bottom-Up Synthesis of High Surface Area Mesoporous Crystalline Silicon and Evaluation of its Hydrogen Evolution performance. *Nature Commun.* **2014**, *5*, 3605.
(6) Zheng, Y.; Jiao, Y.; Zhu, Y.; Li, L. H.; Han, Y.; Chen, Y.; Du, A.; Jaroniec, M.; Qiao, S. Z. Hydrogen Evolution by a Metal-Free Electrocatalyst. *Nature Commun.* **2014**, *5*, 3783−3790.
(7) Morales-Guio, C. G.; Stern, L. A.; Hu, X. Nanostructured Hydrotreating Catalysts for Electrochemical Hydrogen Evolution. *Chem. Soc. Rev.* **2014**, *43*, 6555−6569.
(8) Faber, M. S.; Jin, S. Earth-Abundant Inorganic Electrocatalysts and their Nanostructures for Energy Conversion Applications. *Energy Environ. Sci.* **2014**, *7*, 3519−3542.
(9) Xie, J.; Zhang, J.; Li, S.; Grote, F.; Zhang, X.; Zhang, H.; Wang, R.; Lei, Y.; Pan, B.; Xie, Y. Controllable Disorder Engineering in Oxygen-Incorporated MoS_2 Ultrathin Nanosheets for Efficient Hydrogen Evolution. *J. Am. Chem. Soc.* **2013**, *135*, 17881−17888.
(10) Nocera, D. G. The Artificial Leaf. *Acc. Chem. Res.* **2012**, *45*, 767−776.
(11) Scanlon, M. D.; Bian, X.; Vrubel, H.; Amstutz, V.; Schenk, K.; Hu, X.; Liu, B.; Girault, H. H. Low-Cost Industrially Available Molybdenum Boride and Carbide as "Platinum-Like" Catalysts for the Hydrogen Evolution Reaction in Biphasic Liquid Systems. *Phys. Chem. Chem. Phys.* **2013**, *15*, 2847−2857.
(12) Vrubel, H.; Hu, X. Molybdenum Boride and Carbide Catalyze Hydrogen Evolution in both Acidic and Basic Solutions. *Angew. Chem., Int. Ed.* **2012**, *51*, 12703−12706.
(13) Chen, W.; Sasaki, K.; Ma, C.; Frenkel, A. I.; Marinkovic, N.; Muckerman, J. T.; Zhu, Y.; Adzic, R. R. Hydrogen-Evolution Catalysts Based on Non-Noble Metal Nickel−Molybdenum Nitride Nanosheets. *Angew. Chem., Int. Ed.* **2012**, *51*, 6131−6135.
(14) Sun, Y.; Liu, C.; Grauer, D. C.; Yano, J.; Long, J. R.; Yang, P.; Chang, C. J. Electrodeposited Cobalt-Sulfide Catalyst for Electrochemical and Photoelectrochemical Hydrogen Generation from Water. *J. Am. Chem. Soc.* **2013**, *135*, 17699−17702.
(15) Xie, J.; Li, S.; Zhang, X.; Zhang, J.; Wang, R.; Zhang, H.; Pana, B.; Xie, Y. Atomically-Thin Molybdenum Nitride Nanosheets with Exposed Active Surface Sites for Efficient Hydrogen Evolution. *Chem. Sci.* **2014**, *5*, 4615−4620.
(16) Vrubel, H.; Merki, D.; Hu, X. Hydrogen Evolution Catalyzed by MoS_3 and MoS_2 Particles. *Energy Environ. Sci.* **2012**, *5*, 6136−6144.
(17) Zhuo, S.; Xu, Y.; Zhao, W.; Zhang, J.; Zhang, B. Hierarchical Nanosheet-Based MoS_2 Nanotubes Fabricated by an Anion-Exchange Reaction of MoO_3-Amine Hybrid Nanowires. *Angew. Chem., Int. Ed.* **2013**, *52*, 8602−8606.
(18) Seger, B.; Laursen, A. B.; Vesborg, P. C. K.; Pedersen, T.; Hansen, O.; Dahl, S.; Chorkendorff, I. Hydrogen Production Using a Molybdenum Sulfide Catalyst on a Titanium-Protected n+p-Silicon Photocathode. *Angew. Chem., Int. Ed.* **2012**, *51*, 9128−9131.
(19) Xie, J.; Zhang, H.; Li, S.; Wang, R.; Sun, X.; Zhou, M.; Zhou, J.; Lou, X. W.; Xie, Y. Defect-Rich MoS_2 Ultrathin Nanosheets with Additional Active Edge Sites for Enhanced Electrocatalytic Hydrogen Evolution. *Adv. Mater.* **2013**, *25*, 5807−5813.
(20) Jaramillo, T. F.; Jørgensen, K. P.; Bonde, J.; Nielsen, J. H.; Horch, S.; Chorkendorff, I. Identification of Active Edge Sites for Electrochemical H_2 Evolution from MoS_2 Nanocatalysts. *Science* **2007**, *317*, 100−102.
(21) Lukowski, M. A.; Daniel, A. S.; English, C. R.; Meng, F.; Forticaux, A.; Hamers, R. J.; Jin, S. Highly Active Hydrogen Evolution Catalysis from Metallic WS_2 Nanosheets. *Energy Environ. Sci.* **2014**, *7*, 2608−2613.
(22) Faber, M. S.; Dziedzic, R.; Lukowski, M. A.; Kaiser, N. S.; Ding, Q.; Jin, S. High-Performance Electrocatalysis Using Metallic Cobalt Pyrite (CoS_2) Micro- and Nanostructures. *J. Am. Chem. Soc.* **2014**, *136*, 10053−10061.
(23) Kong, D.; Wang, H.; Lu, Z.; Cui, Y. $CoSe_2$ Nanoparticles Grown on Carbon Fiber Paper: An Efficient and Stable Electrocatalyst for Hydrogen Evolution Reaction. *J. Am. Chem. Soc.* **2014**, *136*, 4897−4900.
(24) Zheng, Y.; Jiao, Y.; Li, L. H.; Xing, T.; Chen, Y.; Jaroniec, M.; Qiao, S. Z. Toward Design of Synergistically Active Carbon-Based Catalysts for Electrocatalytic Hydrogen Evolution. *ACS Nano* **2014**, *8*, 5290−5296.
(25) Popczun, E. J.; McKone, J. R.; Read, C. G.; Biacchi, A. J.; Wiltrout, A. M.; Lewis, N. S.; Schaak, R. E. Nanostructured Nickel Phosphide as an Electrocatalyst for the Hydrogen Evolution Reaction. *J. Am. Chem. Soc.* **2013**, *135*, 9267−9270.
(26) Sakai, T.; Mersch, D.; Reisner, E. Photocatalytic Hydrogen Evolution with a Hydrogenase in a Mediator-Free System under High Levels of Oxygen. *Angew. Chem., Int. Ed.* **2013**, *52*, 12313−12316.
(27) Xu, Y.; Wu, R.; Zhang, J.; Shi, Y.; Zhang, B. Anion-Exchange Synthesis of Nanoporous FeP Nanosheets as Electrocatalysts for Hydrogen Evolution Reaction. *Chem. Commun.* **2013**, *49*, 6656−6658.
(28) Feng, L.; Vrubel, H.; Bensimon, M.; Hu, X. Easily-Prepared Dinickel Phosphide (Ni_2P) Nanoparticles as an Efficient and Robust Electrocatalyst for Hydrogen Evolution. *Phys. Chem. Chem. Phys.* **2014**, *16*, 5917−5921.
(29) Tian, J.; Liu, Q.; Asiri, A. M.; Sun, X. Self-Supported Nanoporous Cobalt Phosphide Nanowire Arrays: An Efficient 3D Hydrogen-Evolving Cathode over the Wide Range of pH 0−14. *J. Am. Chem. Soc.* **2014**, *136*, 7587−7590.
(30) Popczun, E. J.; Read, C. G.; Roske, C. W.; Lewis, N. S.; Schaak, R. E. Highly Active Electrocatalysis of the Hydrogen Evolution Reaction by Cobalt Phosphide Nanoparticles. *Angew. Chem., Int. Ed.* **2014**, *53*, 5427−5430.
(31) Xing, Z.; Liu, Q.; Asiri, A. M.; Sun, X. Closely Interconnected Network of Molybdenum Phosphide Nanoparticles: A Highly Efficient Electrocatalyst for Generating Hydrogen from Water. *Adv. Mater.* **2014**, *26*, 5702−5707.
(32) Tian, J.; Liu, Q.; Cheng, N.; Asiri, A. M.; Sun, X. Self-Supported Cu_3P Nanowire Arrays as an Integrated High-Performance Three-Dimensional Cathode for Generating Hydrogen from Water. *Angew. Chem., Int. Ed.* **2014**, *53*, 9577−9581.
(33) Zou, X.; Huang, X.; Goswami, A.; Silva, R.; Sathe, B. R.; Mikmekova, E.; Asefa, T. Cobalt-Embedded Nitrogen-Rich Carbon Nanotubes Efficiently Catalyze Hydrogen Evolution Reaction at All pH Values. *Angew. Chem., Int. Ed.* **2014**, *53*, 4372−4376.
(34) Liu, Q.; Tian, J.; Cui, W.; Jiang, P.; Cheng, N.; Asiri, A. M.; Sun, X. Carbon Nanotubes Decorated with CoP Nanocrystals: A Highly Active Non-Noble-Metal Nanohybrid Electrocatalyst for Hydrogen Evolution. *Angew. Chem., Int. Ed.* **2014**, *53*, 6710−6714.
(35) Gu, S.; Du, H.; Asiri, A. M.; Sun, X.; Li, C. M. Three-Dimensional Interconnected Network of Nanoporous CoP Nanowires as an Efficient Hydrogen Evolution Cathode. *Phys. Chem. Chem. Phys.* **2014**, *16*, 16909−16913.
(36) Pu, Z.; Liu, Q.; Jiang, P.; Asiri, A. M.; Obaid, A. Y.; Sun, X. CoP Nanosheet Arrays Supported on a Ti Plate: An Efficient Cathode for Electrochemical Hydrogen Evolution. *Chem. Mater.* **2014**, *26*, 4326−4329.
(37) Callejas, J. F.; McEnaney, J. M.; Read, C. G.; Crompton, J. C.; Biacchi, A. J.; Popczun, E. J.; Gordon, T. R.; Lewis, N. S.; Schaak, R. E. Electrocatalytic and Photocatalytic Hydrogen Production from Acidic and Neutral-pH Aqueous Solutions Using Iron Phosphide Nanoparticles. *ACS Nano* **2014**, *8*, 11101−11107.
(38) McEnaney, J. M.; Crompton, J. C.; Callejas, J. F.; Popczun, E. J.; Biacchi, A. J.; Lewis, N. S.; Schaak, R. E. Amorphous Molybdenum Phosphide Nanoparticles for Electrocatalytic Hydrogen Evolution. *Chem. Mater.* **2014**, *26*, 4826−4831.

DOI: 10.1021/am5069547
ACS Appl. Mater. Interfaces 2015, 7, 2376−2384

(39) Shervedani, R. K.; Lasia, A. Kinetics of Hydrogen Evolution Reaction on Nickel−Zinc−Phosphorous Electrodes. *J. Electrochem. Soc.* **1997**, *144*, 2652−2657.
(40) Shervedani, R. K.; Madram, A. R. Electrocatalytic Activities of Nanocomposite $Ni_{81}P_{16}C_3$ Electrode for Hydrogen Evolution Reaction in Alkaline Solution by Electrochemical Impedance Spectroscopy. *Int. J. Hydrogen Energy* **2008**, *33*, 2468−2476.
(41) Zhuo, J.; Wang, T.; Zhang, G.; Liu, L.; Gan, L.; Li, M. Salts of $C_{60}(OH)_8$ Electrodeposited onto a Glassy Carbon Electrode: Surprising Catalytic Performance in the Hydrogen Evolution Reaction. *Angew. Chem., Int. Ed.* **2013**, *52*, 10867−10870.
(42) Subbaraman, R.; Tripkovic, D.; Strmcnik, D.; Chang, K. C.; Uchimura, M.; Paulikas, A. P.; Stamenkovic, V.; Markovic, N. M. Enhancing Hydrogen Evolution Activity in Water Splitting by Tailoring Li^+−$Ni(OH)_2$−Pt Interfaces. *Science* **2011**, *334*, 1256−1260.
(43) Zhang, B.; Ye, X.; Dai, W.; Hou, W.; Xie, Y. Biomolecule-Assisted Synthesis and Electrochemical Hydrogen Storage of Porous Spongelike Ni_3S_2 Nanostructures Grown Directly on Nickel Foils. *Chem.—Eur. J.* **2006**, *12*, 2337−2342.
(44) Zhou, W.; Wu, X.; Cao, X.; Huang, X.; Tan, C.; Tian, J.; Liu, H.; Wang, J.; Zhang, H. Ni_3S_2 Nanorods/Ni Foam Composite Electrode with Low Overpotential for Electrocatalytic Oxygen Evolution. *Energy Environ. Sci.* **2013**, *6*, 2921−2924.
(45) Lu, Z.; Xu, W.; Zhu, W.; Yang, Q.; Lei, X.; Liu, J.; Li, Y.; Sun, X.; Duan, X. Three-Dimensional NiFe Layered Double Hydroxide Film for High-Efficiency Oxygen Evolution Reaction. *Chem. Commun.* **2014**, *50*, 6479−6482.
(46) Chang, Y. H.; Lin, C. T.; Chen, T. Y.; Hsu, C. L.; Lee, Y. H.; Zhang, W.; Wei, K. H.; Li, L. J. Highly Efficient Electrocatalytic Hydrogen Production by MoS_x Grown on Graphene-Protected 3D Ni Foams. *Adv. Mater.* **2013**, *25*, 756−760.
(47) Hu, W. Electrocatalytic properties of new electrocatalysts for hydrogen evolution in alkaline water electrolysis. *Int. J. Hydrogen Energy* **2000**, *25*, 111−118.
(48) McEnaney, J. M.; Crompton, J. C.; Callejas, J. F.; Popczun, E. J.; Read, C. G.; Lewis, N. S.; Schaak, R. E. Electrocatalytic Hydrogen Evolution using Amorphous Tungsten Phosphide Nanoparticles. *Chem. Commun.* **2014**, *50*, 11026−11028.
(49) Henkes, A. E.; Schaak, R. E. Trioctylphosphine: A General Phosphorus Source for the Low-Temperature Conversion of Metals into Metal Phosphides. *Chem. Mater.* **2007**, *19*, 4234−4242.
(50) Guan, Q.; Sun, C.; Li, R.; Li, W. The Synthesis and Investigation of Ruthenium Phosphide Catalysts. *Catal. Commun.* **2011**, *14*, 114−117.
(51) Carenco, S.; Portehault, D.; Boissiere, C.; Mezailles, N.; Sanchez, C. Nanoscaled Metal Borides and Phosphides: Recent Developments and Perspectives. *Chem. Rev.* **2013**, *113*, 7981−8065.
(52) Lu, Z.; Zhu, W.; Yu, X.; Zhang, H.; Li, Y.; Sun, X.; Wang, X.; Wang, H.; Wang, J.; Luo, J.; Lei, X.; Jiang, L. Ultrahigh Hydrogen Evolution Performance of Under-Water "Superaerophobic" MoS_2 Nanostructured Electrodes. *Adv. Mater.* **2014**, *26*, 2683−2687.
(53) Huang, Z.; Chen, Z.; Chen, Z.; Lv, C.; Meng, H.; Zhang, C. $Ni_{12}P_5$ Nanoparticles as an Efficient Catalyst for Hydrogen Generation via Electrolysis and Photoelectrolysis. *ACS Nano* **2014**, *8*, 8121−8129.
(54) Lu, Y.; Tu, J.-P.; Xiong, Q.-Q.; Xiang, J.-Y.; Mai, Y.-J.; Zhang, J.; Qiao, Y.-Q.; Wang, X.-L.; Gu, C.-D.; Mao, S. X. Controllable Synthesis of a Monophase Nickel Phosphide/Carbon (Ni_5P_4/C) Composite Electrode via Wet-Chemistry and a Solid-State Reaction for the Anode in Lithium Secondary Batteries. *Adv. Funct. Mater.* **2012**, *22*, 3927−3935.
(55) Korányi, T. I. Phosphorus Promotion of Ni(Co)-Containing Mo-Free Catalysts in Thiophene Hydrodesulfurization. *Appl. Catal., A* **2003**, *239*, 253−267.
(56) Chen, J.; Zhou, S.; Ci, D.; Zhang, J.; Wang, R.; Zhang, J. Influence of Supports on Structure and Performance of Nickel Phosphide Catalysts for Hydrodechlorination of Chlorobenzene. *Ind. Eng. Chem. Res.* **2009**, *48*, 3812−3819.
(57) Pan, Y.; Liu, Y.; Zhao, J.; Yang, K.; Liang, J.; Liu, D.; Hu, W.; Liu, D.; Liu, Y.; Liu, C. Monodispersed Nickel Phosphide Nanocrystals with Different Phases: Synthesis, Characterization and Electrocatalytic Properties for Hydrogen Evolution. *J. Mater. Chem., A* **2015**, *3*, 1656−1665.
(58) Cruz, M.; Morales, J.; Sánchez, L.; Santos-Peña, J.; Martín, F. Electrochemical Properties of Electrodeposited Nicked Phosphide Thin Films in Lithium Cells. *J. Power Sources* **2007**, *171*, 870−878.
(59) Cecilia, J. A.; Infantes-Molina, A.; Rodríguez-Castellón, E.; Jiménez-López, A. A Novel Method for Preparing an Active Nickel Phosphide Catalyst for HDS of Dibenzothiophene. *J. Catal.* **2009**, *263*, 4−15.
(60) Grosvenor, A. P.; Biesinger, M. C.; Smart, R. S. C.; McIntyre, N. S. New Interpretations of XPS Spectra of Nickel Metal and Oxides. *Surf. Sci.* **2006**, *600*, 1771−1779.
(61) Wehrens-Dijksma, M.; Notten, P. H. L. Electrochemical Quartz Microbalance Characterization of $Ni(OH)_2$-Based Thin Film Electrodes. *Electrochim. Acta* **2006**, *51*, 3609−3621.
(62) Kashani Motlagh, M. M.; Youzbashi, A. A.; Hashemzadeh, F.; Sabaghzadeh, L. Structural Properties of Nickel Hydroxide/Oxyhydroxide and Oxide Nanoparticles Obtained by Microwave-Assisted Oxidation Technique. *Power Technol.* **2013**, *237*, 562−568.
(63) Muthuswamy, E.; Brock, S. L. Oxidation Does Not (Always) Kill Reactivity of Transition Metals: Solution-Phase Conversion of Nanoscale Transition Metal Oxides to Phosphides and Sulfide. *J. Am. Chem. Soc.* **2010**, *132*, 15849−15851.
(64) Kibsgaard, J.; Jaramillo, T. F.; Besenbacher, F. Building an Appropriate Active-Site Motif into a Hydrogen-Evolution Catalyst with Thiomolybdate $[Mo_3S_{13}]^{2-}$ Clusters. *Nature Chem.* **2014**, *6*, 248−253.
(65) Chen, L.; Wang, M.; Han, K.; Zhang, P.; Gloaguen, F.; Sun, L. A Super-Efficient Cobalt Catalyst for Electrochemical Hydrogen Production from Neutral Water with 80 mV Overpotential. *Energy Environ. Sci.* **2014**, *7*, 329−334.
(66) Li, Y.; Wang, H.; Xie, L.; Liang, Y.; Hong, G.; Dai, H. MoS_2 Nanoparticles Grown on Graphene: An Advanced Catalyst for the Hydrogen Evolution Reaction. *J. Am. Chem. Soc.* **2011**, *133*, 7296−7299.
(67) Chang, J.; Feng, L.; Liu, C.; Xing, W.; Hu, X. An Effective Pd−Ni_2P/C Anode Catalyst for Direct Formic Acid Fuel Cells. *Angew. Chem., Int. Ed.* **2014**, *53*, 122−126.
(68) Bag, S.; Gaudette, A. F.; Bussell, M. E.; Kanatzidis, M. G. Spongy Chalcogels of Non-Platinum Metals Act as Effective Hydrodesulfurization Catalysts. *Nature Chem.* **2009**, *1*, 217−224.
(69) Miao, S.; Hickey, S. G.; Rellinghaus, B.; Waurisch, C.; Eychmüller, A. Synthesis and Characterization of Cadmium Phosphide Quantum Dots Emitting in the Visible Red to Near-Infrared. *J. Am. Chem. Soc.* **2010**, *132*, 5613−5615.
(70) Miao, S.; Hickey, S. G.; Waurisch, C.; Lesnyak, V.; Otto, T.; Rellinghaus, B.; Eychmüller, A. Synthesis of Monodisperse Cadmium Phosphide Nanoparticles Using ex Situ Produced Phosphine. *ACS Nano* **2012**, *6*, 7059−7065.
(71) Wang, F.; Li, C.; Li, Y.; Yu, J. C. Hierarchical P/YPO_4 Microsphere for Photocatalytic Hydrogen Production from Water under Visible Light Irradiation. *Appl. Catal., B* **2012**, *119−120*, 267−272.
(72) Wang, F.; Ng, W. K. H.; Yu, J. C.; Zhu, H.; Li, C.; Zhang, L.; Liu, Z.; Li, Q. Red Phosphorus: An Elemental Photocatalyst for Hydrogen Formation from Water. *Appl. Catal., B* **2012**, *111−112*, 409−414.

DOI: 10.1021/am5069547
ACS Appl. Mater. Interfaces 2015, 7, 2376−2384